Dual n- and p-Type Dopable Electrochromic Devices Employing Transparent Carbon Nanotube Electrodes

ARTICLE *in* CHEMISTRY OF MATERIALS · NOVEMBER 2009

Impact Factor: 8.35 · DOI: 10.1021/cm902768q

9 AUTHORS, INCLUDING:

Aubrey Dyer
Georgia Institute of Technology
32 PUBLICATIONS **1,221** CITATIONS
SEE PROFILE

Timothy Steckler
Chalmers University of Technology
24 PUBLICATIONS **532** CITATIONS
SEE PROFILE

Zhuangchun wu
Nanjing University of Science and Technology
51 PUBLICATIONS **2,628** CITATIONS
SEE PROFILE

David Tanner
University of Florida
503 PUBLICATIONS **12,052** CITATIONS
SEE PROFILE

CHEMISTRY OF MATERIALS
Article

Chem. Mater. **XXXX,** *XXX,* 000–000 A
DOI:10.1021/cm902768q

Dual *n*- and *p*-Type Dopable Electrochromic Devices Employing Transparent Carbon Nanotube Electrodes

Maria Nikolou,[†] Aubrey L. Dyer,*[,‡] Timothy T. Steckler,[‡] Evan P. Donoghue,[†] Zhuangchun Wu,[†] Nathan C. Heston,[†] Andrew G. Rinzler,[†] David B. Tanner,[†] and John R. Reynolds[‡]

[†]*Department of Physics and* [‡]*The George and Josephine Butler Polymer Laboratories, Department of Chemistry, Center for Macromolecular Science and Engineering, University of Florida, Gainesville, Florida 32611*

Received September 4, 2009. Revised Manuscript Received October 6, 2009

We report on the use of highly transmissive single-walled carbon nanotube (SWNT) films as electrodes in electrochromic devices that employ a dual *n*- and *p*-type dopable donor−acceptor polymer, poly[5,8-bis-(3-dihydro-thieno[3,4-*b*][1,4]dioxin-5-yl)-2,3-diphenyl-pyrido[3,4-*b*]pyrazine], or poly-(bisEDOT-PyrPyr-Hx$_2$). This low bandgap polymer is capable of repeated, stable electrochemical cycling between a neutral form and both an oxidized, *p*-doped state and a reduced, *n*-doped state. The ability of this electrochromic material to exhibit a stable *n*-type doped state enabled the construction of an absorptive/transmissive dual-window electrochromic device showing optical changes over a broad energy range—from the mid-infrared to the visible region. This absorptive/transmissive dual polymer electrochromic device is unique in that it exhibits electrochromism utilizing the same polymer as both the cathodically and anodically coloring material. Infrared electrochromic behavior was achieved with the use of SWNT films due to their high transmissivity in the near to mid-IR (1−3 μm). Initial results studying the long-term redox switching stability of the absorptive/transmissive poly(bisEDOT-PyrPyr-Hx$_2$) ECD demonstrate that the system can be repeatedly cycled (> 2,000 cycles) and maintain a high optical contrast in the near-infrared (32% at 2000 nm).

Introduction

Conjugated electroactive polymers have been employed in diverse applications, many of which utilize the polymer in the neutral form, such as thin film transistors, light-emitting diodes, and photovoltaic devices. Other applications include those that utilize the polymer as a redox-active material such as sensors, antistatic coatings, batteries, supercapacitors, and electrochromic devices.[1] With a high-lying HOMO (highest occupied molecular orbital), the majority of conjugated polymers exhibit *p*-type doping at fairly low oxidation potentials. Systems that exhibit *n*-type doping are less commonly obtained due to practically inaccessible reduction potentials and instability of organic anions, especially to water and oxygen.[2−6] The availability of a dual *n*- and *p*-dopable polymer with a low oxidation potential, in addition to a relatively positive reduction potential, would be beneficial in the construction of redox-active devices where the same electroactive polymer is present at both the anode and the cathode. One such device is a dual-polymer absorptive/transmissive electrochromic device. In this instance, the single polymer serves as both the cathodically and anodically coloring films on the respective sides of the device. This concept is similar to those employed in Type III supercapacitors where the anode and cathode sides are symmetric, utilizing the same polymer as both the *n*-doping material and the *p*-doping material.[7] This approach has advantages over other, asymmetric devices in that there is no inherent polarity (i.e., there is no difference in how the device is connected) and there is a larger operating voltage range.

It has been previously shown that low bandgap donor−acceptor (D/A) polymers have unique redox properties among conjugated polymers because of their ability to reach multiple electronic states (e.g., *p*-type and *n*-type doping) in a small potential window.[8−10] The approach to making these polymers is to couple a strong donor (high

*Corresponding author. E-mail: adyer@chem.ufl.edu. Phone: (352) 392-2012. Fax: (352) 392-9741.

(1) *Handbook of Conducting Polymers*, 3rd ed.; Skotheim, T. A., Reynolds, J. R., Eds.; CRC Press: Boca Raton, FL, 2007.
(2) Zotti, G.; Schiavon, G.; Zecchin, S. *Synth. Met.* **1995**, *72*, 275.
(3) De Leeuw, D. M.; Simenon, M. M. J.; Brown, A. R.; Einerhand, R. E. F. *Synth. Met.* **1997**, *87*, 53.
(4) Chiechi, R. C.; Sonmez, G.; Wudl, F. *Adv. Funct. Mater.* **2005**, *15*, 427.
(5) Witker, D. L.; Cleancy, S. O.; Irvin, D. J.; Stenger-Smith, J. D.; Irvin, J. A. *J. Electrochem. Soc.* **2007**, *154*, G95.
(6) Bourgeaux, M.; Skene, W. G. *Macromolecules* **2007**, *40*, 1792.
(7) Irvin, J. A.; Irvin, D. J.; Stenger-Smith, J. D. Electroactive Polymers for Batteries and Supercapactiors. In *Handbook of Conducting Polymers*, 3rd ed.; Skotheim, T. A., Reynolds, J. R., Eds.; CRC Press: Boca Raton, FL, 2007.
(8) DuBois, C. J.; Reynolds, J. R. *Adv. Mater.* **2002**, *14*, 1844.
(9) Irvin, D. J.; DuBois, C. J.; Reynolds, J. R. *Chem. Commun.* **1999**, 2121.
(10) DuBois, C. J.; Abboud, K. A.; Reynolds, J. R. *J. Phys. Chem. B.* **2004**, *108*, 8550.

Scheme 1

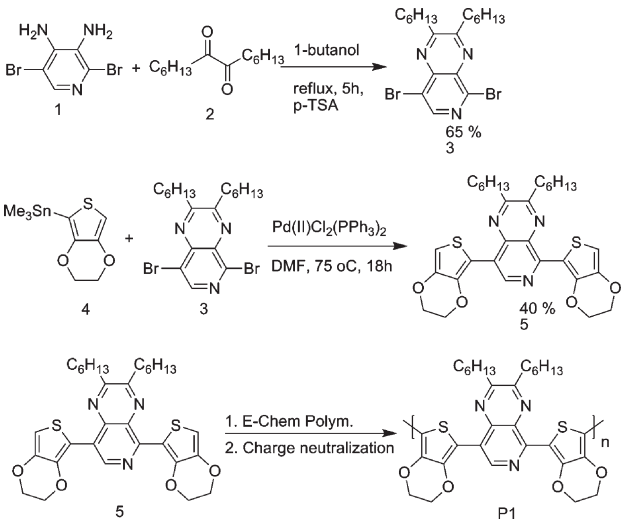

HOMO level) to a strong acceptor (low LUMO level), with the newly formed D/A complex HOMO taking on a similar energy to the donor, while the LUMO will be similar in energy to the acceptor. As such, the new donor−acceptor material has a reduced bandgap (E_g) relative to either of its parent components.[11−17]

These low bandgap polymers are typically colored in their neutral state as their $\pi-\pi^*$ transition lies in the visible or even the near-infrared region of the electromagnetic spectrum. The materials become more transparent to the eye upon doping, as the $\pi-\pi^*$ transition is bleached and lower-energy electronic transitions, which absorb in the IR, develop. One such material, the donor−acceptor polymer, poly[5,8-bis-(3-dihydro-thieno[3,4-*b*]-[1,4]dioxin-5-yl)-2,3-diphenyl-pyrido[3,4-*b*]pyrazine] [poly-(bisEDOT-PyrPyr-Hx$_2$)] with the repeat unit shown in Scheme 1 has access to four different electronic states (neutral and oxidized, along with singly and doubly reduced).[8,10,18] The use of 3,4-ethylenedioxythiophene (EDOT) as the terminal heterocycle in the monomer takes advantage of its low oxidation potential for ease of electrochemical polymerization and yields a BiEDOT donor positioning a high HOMO level in the polymer. The pyridopyrazine acceptor moiety allows access to the multiple reductive states, which can lead to novel devices as it is capable of accepting two negative charges.

The study of the electrochromism of low bandgap polymers, such as the D/A systems described, has been hindered by the limited availability of electrodes possessing transparency from the visible through the mid-infrared regions of the spectrum. The commonly used transparent electrode, indium tin oxide on glass (ITO/glass), has excellent transmissivity in the visible region but drops off dramatically beyond 1200 nm. To characterize the large near to mid-IR contrasts available in conjugated conducting polymers and capitalize on this in electrochromic applications, an electrode material retaining transparency to wavelengths of 10 μm is necessary. Wu et al. first demonstrated that continuous films of purified single-walled carbon nanotubes (SWNTs) made thinner than ~300 nm could serve as transparent electrodes over the relevant spectral range.[11,19] The optical transmittance and electrical resistance of such films are a function of the inverse of film thickness requiring a compromise between the desired high transmittance and low sheet resistance. The severity of this compromise depends on the quality of the SWNTs used, in terms of their mean lengths, defect density and purity, and the charge-transfer-doping state of the nanotubes. In the present studies, SWNTs grown by pulsed laser vaporization at 1100 °C, charge-transfer-doped during their nitric acid based purification, gave, for 60 nm thick films, a transmittance across the visible spectrum > 60% and a low sheet resistance of ~60 Ω/□.[20] The spectral transmittance of the films improves in the IR peaking at over 90% in a broad maximum centered at ~2200 nm while falling only to ~70% at 10 μm.

Electrochromic devices (ECDs) operating in the mid-infrared region are potentially important in applications that require dynamic control of thermal emissivity such as in building construction, automotive, and aerospace applications, among others. The most commonly reported electrochromic devices operating in the long wavelength regions are those that are absorptive/reflective-based.[21−25] These devices contain an electrochromic polymer coated on a porous reflective metal. The IR radiation is modulated as it passes through the electroactive polymer and is reflected by the metallic surface. While these devices have successfully demonstrated modulation in the reflective mode from 0.3 μm to greater than 20 μm, there is a strong need for absorptive/transmissive window-type ECDs that can operate effectively across the long wavelength regions and can give both visible and infrared light modulation.

In this work, we present the electrochemical characterization of a dual *n*- and *p*-type dopable D/A electrochromic polymer, poly(bisEDOT-PyrPyr-Hx$_2$), on glassy

(11) Steckler, T. T.; Abboud, K. A.; Craps, M.; Rinzler, A. G.; Reynolds, J. R. *Chem. Commun.* **2007**, 4904.
(12) Van Mullekom, H. A. M.; Vekemans, J. A. J. M.; Havinga, E. E.; Meijer, E. W. *Mater. Sci. Eng.* **2001**, *32*, 1.
(13) Roncali, J. *Chem. Rev.* **1997**, *97*, 173.
(14) Bundgaard, E.; Krebs, F. C. *Macromolecules* **2006**, *39*, 2823.
(15) Dhanabalan, A.; Van Duren, J. K. J.; Van Hal, P. A.; Van Dongen, J. L. J.; Janssen, R. A. J. *Adv. Funct. Mater.* **2001**, *11*, 255.
(16) Brabec, C. J.; Winder, C.; Sariciftci, N. S.; Hummelen, J. C.; Dhanabalan, A.; Van Hal, P. A.; Janssen, R. A. J. *Adv. Funct. Mater.* **2002**, *12*, 709.
(17) Zoombelt, A. P.; Fonrodona, M.; Wienk, M. M.; Sieval, A. B.; Hummelen, J. C.; Janssen, R. A. J. *Org. Lett.* **2009**, *11*, 903.
(18) Lee, B. −L.; Yamamoto, T. *Macromolecules* **1999**, *32*, 1375.
(19) Wu, Z.; Chen, Z.; Du, X.; Logan, J. M.; Nikolou, M.; Kamaras, K.; Reynolds, J. R.; Tanner, D. B.; Hebard, A. F.; Rinzler, A. G. *Science* **2004**, *305*, 1273.
(20) Rinzler, A. G.; Liu, J.; Dai, H.; Nikolaev, P.; Huffman, C. B.; Rodriguez-Macias, F. J.; Boul, P. J.; Lu, A. H.; Heymann, D.; Colbert, D. T.; Lee, R. S.; Fischer, J. E.; Rao, A. M.; Eklund, P.; Smalley, R. E. *Appl. Phys. A: Mater. Sci. Process.* **1998**, *67*, 29.
(21) Bennett, R. N.; Kokonaski, W. E.; Hannan, M. J.; Boxall, L. G., Electrode for Display Devices. U.S. Patent 5,445,577, August **1995**.
(22) Chandrasekhar, P.; Zay, B. J.; Birur, G. C.; Rawal, S.; Pierson, E. A.; Kauder, L.; Swanson, T. *Adv. Funct. Mater.* **2002**, *12*, 95.
(23) Schwendeman, I.; Hwang, J.; Welsh, D. M.; Tanner, D. B.; Reynolds, J. R. *Adv. Mater.* **2001**, *13*, 634.
(24) Chandrasekhar, P. Electrochromic Display Device. U.S. Patent 5,995,273, November **1999**.
(25) Dyer, A. L.; Grenier, C. R. G.; Reynolds, J. R. *Adv. Funct. Mater.* **2007**, *17*, 1480.

carbon button electrodes in addition to spectroelectrochemical results over a broad range of the electromagnetic spectrum. Importantly, this includes a comparison of results for the low bandgap polymer deposited as thin films on both ITO and SWNTs on glass substrates. Furthermore, a description of two types of absorptive/transmissive devices that operate in the visible, near-infrared, and mid-infrared regions is presented. The construction of these devices was possible due to the availability of two novel materials; the low bandgap polymer poly(bisEDOT-PyrPyr-Hx_2) and visible light to near- and mid-infrared transparent conducting SWNT films.

Experimental Section

Materials. Tetrabutylammonium perchlorate (TBAP) was prepared from tetrabutylammonium bromide and perchloric acid and recrystallized (3 times) from absolute ethanol. Propylene carbonate (PC) was purchased from Acros and distilled under reduced pressure with the second fraction collected. Dichloromethane (DCM) was passed through a MBraun solvent purification system that renders the solvent dry on retrieval. All purified solvents were deoxygenated by repeated freeze−pump−thaw cycles before use. ITO/glass electrodes were obtained from Delta Technologies, Ltd., and rinsed with distilled water followed by isopropanol before use. Gold-coated (100 nm thick) Kapton sheets (Astral Technologies Unlimited) were cut to shape with scissors and used as received. Transparent conductive films of single-walled carbon nanotubes (SWNTs) were made via the vacuum filtration method described previously[19] resulting in SWNT films 60 nm thick with sheet resistances of 60 Ω/□. These films were subsequently transferred to cleaned glass slides or poly(ethylene terephthalate) (PET, Dura-lar) on which palladium contact electrodes had been predeposited.

Synthesis. 3,4-Diamino-2,5-dibromopyridine (**1**), tetradecane-7,8-dione (**2**), and 2,3-dihydrothieno[3,4-*b*][1,4]dioxin-5-yl trimethylstannane ($EDOTSn(CH_3)_3$) (**4**) were prepared according to literature methods.[18,26,27]

5,8-Dibromo-2,3-dihexyl-pyrido[3,4-b]pyrazine (*3*). 3,4-Diamino-2,5-dibromopyridine (1.31 g, 4.9 mmol), tetradecane-7,8-dione (1.14 g, 5.0 mmol), *p*-toluenesulfonic acid monohydrate (0.02 g, 0.10 mmol), and 20 mL of 1-butanol were combined in a 100 mL 3-neck round-bottom flask equipped with a reflux condenser and stir bar. The solution was then heated to reflux for 5 h. After cooling, a precipitate was collected by filtration. Recrystallization from EtOH yielded 1.46 g (65%) of an off-white solid. Mp 71.5−72.8 °C. ^{1}H NMR (300 MHz, $CDCl_3$) δ 0.92 (t, 6H, $J = 7$ Hz), 1.3−1.5 (m, 12H), 1.92 (m, 4H), 3.10 (m, 4H), 8.68 (s, 1H); ^{13}C NMR (75 MHz, $CDCl_3$) δ 14.1, 22.6, 22.6, 27.4, 29.1, 29.1, 31.6, 31.7, 34.8, 35.1, 120.1, 136.0, 142.5, 145.7, 146.4, 160.5, 163.2. Elemental Anal. Calcd for $C_{19}H_{27}N_3Br_2$: C, 49.91; H, 5.95; N, 9.19; Br, 34.95. Found: C, 50.03; H, 5.99; N, 9.06. HRMS calcd for $C_{19}H_{27}N_3Br_2$, 457.0551; found, 457.0556.

5,8-Bis(2,3-dihydrothieno[3,4-b][1,4]dioxin-5-yl)-2,3-dihexyl-pyrido[3,4-b]pyrazine (*5*). Under an argon atmosphere, 5,8-dibromo-2,3-dihexyl-pyrido[3,4-*b*]pyrazine (0.42 g, 0.92 mmol), (2,3-dihydrothieno[3,4-*b*][1,4]dioxin-5-yl)trimethylstannane (0.66 g, 2.0 mmol), and 25 mL of anhydrous DMF were combined in a dry 100 mL 3-neck round-bottom flask with a stir bar. The mixture was degassed under argon for 1 h. Then $Pd(II)Cl_2(PPh_3)_2$ (0.07 g, 11 mol %) was added, and the solution was heated to 75 °C and allowed to react for ~18 h. After cooling, the reaction mixture was poured into 200 mL of H_2O and extracted repeatedly with ether. The organic solution was then concentrated and extracted repeatedly with brine. After drying over $MgSO_4$, removal of ether under reduced pressure gave an orange-red solid. Column chromatography (1:1 DCM:EtOAc) yielded 0.21 g (40%) of an orange crystalline powder. Mp 167−168 °C. ^{1}H NMR (300 MHz, $CDCl_3$) δ 0.91 (t, 6H, $J =$ 6 Hz), 1.3−1.55 (m, 12H), 1.95−2.1 (m, 4H), 3.00−3.15 (m, 4H), 4.25−4.50 (m, 8H), 6.55 (s, 1H), 6.63 (s, 1H), 9.72 (s, 1H); ^{13}C NMR (75 MHz, $CDCl_3$) δ 14.1, 22.6, 27.6, 27.7, 29.2, 31.8, 34.9, 35.2, 64.2, 64.3, 64.8, 65.3, 103.1, 105.2, 110.9, 114.0, 122.3, 132.5, 139.5, 140.4, 141.3, 141.7, 142.5, 144.3, 149.8, 156.1, 159.2. Elemental Anal. Calcd for $C_{31}H_{37}N_3O_4S_2$: C, 64.22; H, 6.47; N, 7.25. Found: C, 64.21; H, 6.68; N, 7.19. HRMS calcd for $C_{31}H_{37}N_3O_4S_2$, 579.2225; found, 579.2210.

Electrochemistry. All electrochemical experiments were performed in a 3-electrode electrochemical cell using an EG&G PAR model 273A potentiostat/galvanostat with the electrochemical cell located in a controlled-atmosphere glovebox with O_2 levels less than 4 ppm and moisture content less than 1 ppm. Electrochemical polymerization of the monomer BEDOT-Pyr-Pyr-$(C_6H_{13})_2$ was performed from a solution containing 10 mM monomer in 0.2 M TBAP in a 3:1 propylene carbonate:dichloromethane mixture by cyclic voltammetry or potentiostatically (~0.95 V vs Fc/Fc^+) until a desired charge passed. The resulting films on ITO or SWNT are typically in the 150−200 nm thickness range as measured by profilometry. The 3-electrode configuration used for the film deposition consisted of the working electrode (either glassy carbon button, ITO/glass, SWNT on glass or PET, or Au/Kapton), a platinum (Pt) flag as the counter electrode, and a silver (Ag) wire pseudoreference calibrated with the Fc/Fc^+ redox couple. After the film growth, the polymer-coated electrodes were removed from the monomer solution and rinsed with solvent (PC). Further electrochemistry on the polymer films were performed in an electrolyte solution containing 0.2 M TBAP in PC.

Spectroscopy. In situ spectroelectrochemistry was performed using a Cary 500 UV/Vis-NIR spectrophotometer with a measurement range that extended from 200 nm in the UV to 3300 nm in the NIR. The polymer films were polymerized onto transparent electrodes of either ITO/glass or SWNT/glass and placed in a quartz cuvette fitted with a Teflon cap (fabricated in-house) that allowed for placement of the transparent electrode, Pt wire counter electrode, and Ag wire pseudoreference (calibrated with the Fc/Fc^+ redox standard). The cuvette was filled with supporting electrolyte and the cell sealed with Teflon tape. The spectroelectrochemical cell was assembled in the inert atmosphere glovebox and sealed before placement in the spectrophotometer. The sealing of the electrochemical cell prevents the entrance of moisture or oxygen once the cell is removed from the glovebox during spectroscopic measurements. In the case of the electrochromic devices, the spectrophotometer was fitted with a flat plate holder onto which the device was mounted to hold the device normal to the incident light beam.

Electrochromic Device Construction. Two different device designs were utilized to allow measurement of the long wavelength optical contrasts. The working electrode in all devices consisted of a SWNT film (60 nm ± 10 nm) on either plastic or glass substrate. The dual window ECD contained two SWNT electrodes for both the working and counter electrodes.

(26) Srinivasan, N. S.; Lee, D. G. *J. Org. Chem.* **1979**, *44*, 1574.
(27) Wang, F.; Wilson, M. S.; Rauh, R. D.; Schottland, P.; Thompsono, B. C.; Reynolds, J. R. *Macromolecules* **2000**, *33*, 2083.

The single-window ECD was composed of a SWNT/PET electrode as the working electrode and a gold-coated (100 nm thick) Kapton sheet as the counter electrode. To probe the spectral response of the polymer at the SWNT/PET working electrode, a hole of 3−4 mm diameter was cut into the Au/Kapton electrode through which the light beam from the spectrometer would pass. The hole was sealed with an infrared transmissive PET window. Before assembly, the electrodes were coated with a thin layer of gel electrolyte that contained 10 mL of PC, 1.1 g of PMMA, and 0.5 M TBAP. The electrodes were then sandwiched together and sealed with epoxy. Preparation, assembly, and encapsulation of the devices took place in the inert atmosphere glovebox.

Results and Discussion

Synthesis of BisEDOT-PyrPyr-Hx$_2$. Preparation of the D/A monomer (as is shown in Scheme 1) starts with formation of the acceptor moiety 5,8-dibromo-2,3-dihexylpyrido[3,4-*b*]pyrazine: Br_2Pyr-Pyr-(C_6H_{13})$_2$ (**3**). First, 3,4-diamino pyridine was brominated at the 2 and 5 positions with bromine in 48% HBr to yield 3,4-diamino-2,5-dibromopyridine (**1**).[18] This provides the base of the acceptor unit which can then be functionalized with α-diones. Tetradecane-7,8-dione (**2**) was prepared by oxidation of 7-tetradecyne with $KMnO_4$ in acetone/H_2O.[26] Finally, Br_2Pyr-Pyr-(C_6H_{13})$_2$ was obtained by condensation between 3,4-diamino-2,5-dibromopyridine and tetradecane-7,8-dione in refluxing butanol.[18] 2,3-Dihydrothieno[3,4-*b*][1,4]dioxin-5-yl trimethylstannane (EDOTSn(CH_3)$_3$) (**4**) was chosen as the donor due to its ability to be isolated and purified before coupling.[27] A Stille cross-coupling reaction between the donor, EDOTSn(CH_3)$_3$, and the acceptor, Br_2Pyr-Pyr-(C_6H_{13})$_2$, yielded 5,8-bis-(2,3-dihydrothieno[3,4-*b*][1,4]dioxin-5-yl)-2,3-dihexyl-pyrido[3,4-*b*]pyrazine (BEDOT-PyrPyr-(C_6H_{13})$_2$) (**5**) in moderate yields. The monomer was characterized by ^{1}H and ^{13}C NMR spectroscopy, elemental analysis, and high-resolution mass spectrometry.

Electrochemistry. Poly(bisEDOT-PyrPyr-Hx$_2$) films were prepared by electrochemical polymerization and concurrent deposition onto glassy carbon working electrodes by cyclic voltammetry to characterize both the monomer oxidation potential and the polymer electrochemistry during film deposition as is shown in Figure 1. The monomer exhibits an oxidation onset at 0.57 V vs Fc/Fc$^+$ and a peak oxidation potential at 0.67 V vs Fc/Fc$^+$ as can be seen in the figure inset. On repeated cycling, polymer oxidation and neutralization at the electrode occurs, resulting in polymer film deposited on the electrode surface.

The polymer-coated electrode was removed from the monomer solution and rinsed with PC before being immersed in an electrolyte solution containing 0.2 M TBAP in PC. The polymer electrochemistry was then examined by first oxidatively cycling the polymer film for multiple scans to characterize *p*-doping, followed by reductive cycling to probe the *n*-doping properties of the film. The results are given in Figure 2. The polymer has a very broad oxidation profile with a slight peak at 0.19 V vs Fc/Fc$^+$. The *n*-doping process was more clearly defined with a reduction peak at −1.69 V and an onset to reduction at −1.48 V vs Fc/Fc$^+$.

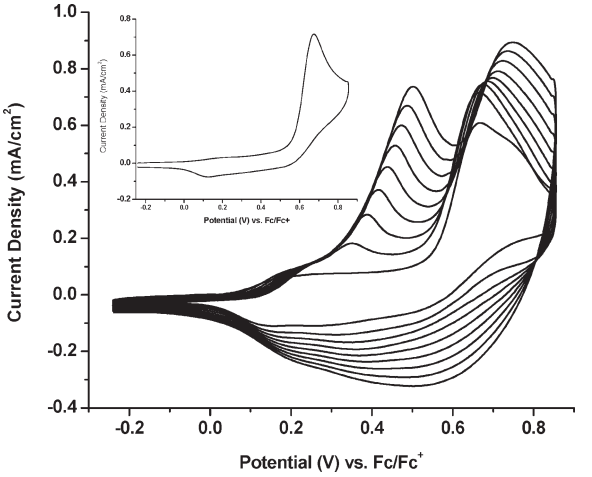

Figure 1. Electropolymerization of bisEDOT-PyrPyr-Hx$_2$ on a glassy carbon button electrode. Polymerization was performed in a 10 mM monomer, 0.2 M TBAP, 3:2 PC:DCM solution at a scan rate of 50 mV/s for 10 cycles. The inset shows the first scan CV.

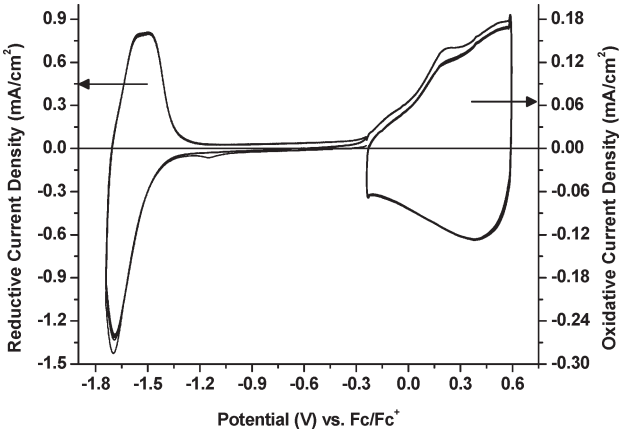

Figure 2. Repeated cycling of poly(bisEDOT-PyrPyr-Hx$_2$) film on glassy carbon electrode. The polymer is first cycled oxidatively (positive potentials) and then reductively (negative potentials) at 50 mV/s in 0.2 M TBAP/PC electrolyte.

During the first reduction scan, a small peak at −1.1 V is seen and is attributed to trapped charges that are expelled and is no longer present on repeated scans.[28] The polymer does have a second reduction at a further negative potential (not shown) that is, however, unstable with the polymer losing electroactivity upon accessing that second reduction. In addition to being more clearly defined, the reduction process also occurs with a much larger current density than the oxidation process as can be noted by the five times larger current density for *n*-doping than for *p*-doping and a three times larger charge density (not shown). This behavior has been noted previously in similar systems and is attributed to both *n*-doping and a redox transport mechanism with the lack of a capacitive character indicative of a localized anionic state rather than the delocalized state required for significant *n*-type conductivity.[8,10]

(28) Thomas, C. A.; Zong, K.; Abboud, K. A.; Stell, P. J.; Reynolds, J. R. *J. Am. Chem. Soc.* **2004**, *126*, 16440.

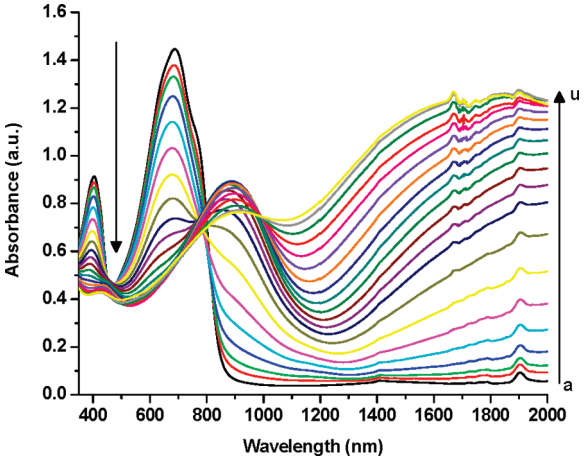

Figure 3. Spectroelectrochemistry of a poly(bisEDOT-PyrPyr-Hx$_2$) film grown potentiostatically to 40 mC on ITO/glass between the applied potentials of (a) −1.1 V and (b−u) −0.25 V to 0.7 V in 0.05 V increments vs Fc/Fc$^+$.

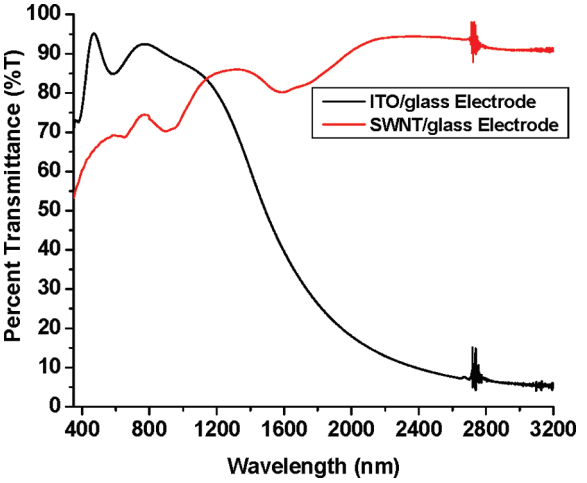

Figure 4. Transmittance spectra of ITO/glass (~10 Ω/□) and SWNT/glass (~60 Ω/□) illustrating the large transmittance window of the SWNT films in the NIR and mid-IR regions of the spectrum.

Spectroelectrochemistry on ITO/Glass. Films of poly(bisEDOT-PyrPyr-Hx$_2$) were electrodeposited onto ITO/glass potentiostatically at +0.8 V vs Fc/Fc$^+$ from 10 mM monomer and 0.2 M TBAP in a solvent containing DCM:PC in a 2:3 ratio. The films were then rinsed in dry PC and placed in an electrolyte solution of 0.2 M TBAP/PC for spectroelectrochemical measurements. Before measurements were taken, the film was held at a neutralizing potential of −1.0 V vs Fc/Fc$^+$ for approximately 10 min. The in situ spectroelectrochemistry was performed by holding the film at the desired potential and measuring the absorbance from 350 to 2000 nm with applied potentials ranging from −1.0 to 0.7 V vs Fc/Fc$^+$ for *p*-doping. The polymer switches from a dark teal-green in the neutral state to a slate-blue in the oxidized state. As can be seen in Figure 3, the polymer has two absorbance bands in the visible region, characteristic of donor−acceptor systems. A window of transmission is centered around 500 nm and gives the polymer a green color as the green light is not absorbed and is allowed to pass through the film. The polymer has a bandgap (absorption onset), at 860 nm, corresponding to 1.4 eV with a λ_{max} at 687 nm, and a lower intensity absorption maximum at 400 nm. As the polymer is oxidized, depletion of both of these transitions occurs with a decrease in the absorbances at 687 and 400 nm. The doping-induced infrared absorption bands begin to emerge at intermediate oxidation levels with an absorbance centered at 900 nm and a broad absorbance beginning at 1200 nm and extending into the mid-IR.

While ITO/glass electrodes are sufficiently transparent in the visible region, their transmission window drops off substantially at longer wavelengths, as can be seen in Figure 4. The ITO utilized in this study (10 Ω/□) has a transmittance value of 50% at 1490 nm, reduced to 18% at 2000 nm, the limiting wavelength for solution-based spectroelectrochemistry. It should be noted that the ability to measure the optical transitions of the polymer film on ITO in Figure 3 was made possible by the use of a dual-beam spectrophotometer that can effectively subtract the large absorbances of the substrate. However, for practical applications in the IR, an electrode material with higher near- to mid-IR transparency is required. For this application, we have utilized SWNT/glass electrodes that were demonstrated previously to have sufficient transmittance at longer wavelengths as shown in Figure 4. The SWNT films chosen for this study have a sheet resistance of 60 Ω/□ and transmittance greater than 90% from 2000 to 3200 nm (the wavelength limit of the spectrophotometer used here). While the transmittance of these films is less than that of ITO in the visible region, it never drops below 60% when measured from 400 to 1100 nm. The remaining spectroelectrochemical measurements of the polymer film alone and in ECDs were then performed on these SWNT/glass electrodes as is shown in the following sections.[29−31]

Spectroelectrochemistry on SWNT/Glass Electrodes. Because electrochromic device fabrication and characterization were to be performed using IR transmissive SWNT/glass electrodes as the transparent conductor, it was necessary that poly(bisEDOT-PyrPyr-Hx$_2$) film optical characterization be performed on these electrodes alone to allow a direct comparison. As with the ITO/glass electrodes, electropolymerization was performed potentiostatically from a monomer solution containing 0.2 M TBAP in a mixed solvent of 2:3 DCM:PC. In situ spectroelectrochemistry was performed during *p*-doping and *n*-doping for the polymer film and is shown in Figure 5A,B.

As with the polymer film on ITO, potentials from −1.0 to 0.7 V vs Fc/Fc$^+$ were applied to the electrode, and a decrease in the $\pi-\pi^*$ transition occurs at the expense of the lower energy electronic transitions with large contrasts in the NIR to 2000 nm. Specifically, absorption in the visible region begins to decrease as the absorptions in the NIR begin to increase at voltages greater than −0.3 V vs Fc/Fc$^+$. This can be more clearly seen in Figure 6A where absorbances at wavelengths in the visible (695 nm)

(29) Hu, L.; Gruner, G.; Li, D.; Kaner, R. B.; Cech, J. *J. Appl. Phys.* **2007**, *101*, 1.
(30) Jain, V.; Yochum, H. M.; Montazami, R.; Heflin, J. R.; Hu, L.; Gruner, G. *J. Appl. Phys.* **2008**, *103*, 1.
(31) Vasilyeva, S.; Unur, E., Walczak, R. M.; Donoghue, E.; Rinzler, A. G.; Reynolds, J. R. *ACS Appl. Mater. Interfaces* **2009**, accepted.

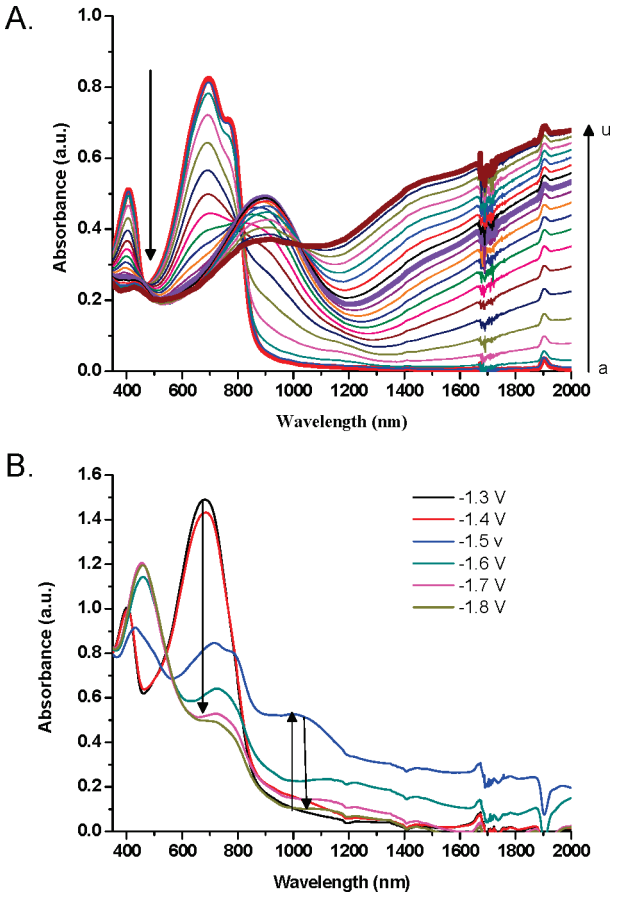

Figure 5. In situ spectroelectrochemistry of poly(bisEDOT-PyrPyr-Hx$_2$) on a SWNT/glass electrode switched in 0.2 M TBAP/PC on (A) *p*-doping and (B) *n*-doping. Potentials given are versus Fc/Fc$^+$. Potentials for *p*-doping are at the applied potentials of (a) −1.1 V and (b−u) −0.25 V to 0.7 V in 0.05 V increments vs Fc/Fc$^+$. The thicker lines in the top graph indicate when the film is fully neutralized (pink), partially oxidized (purple), and fully oxidized (brown).

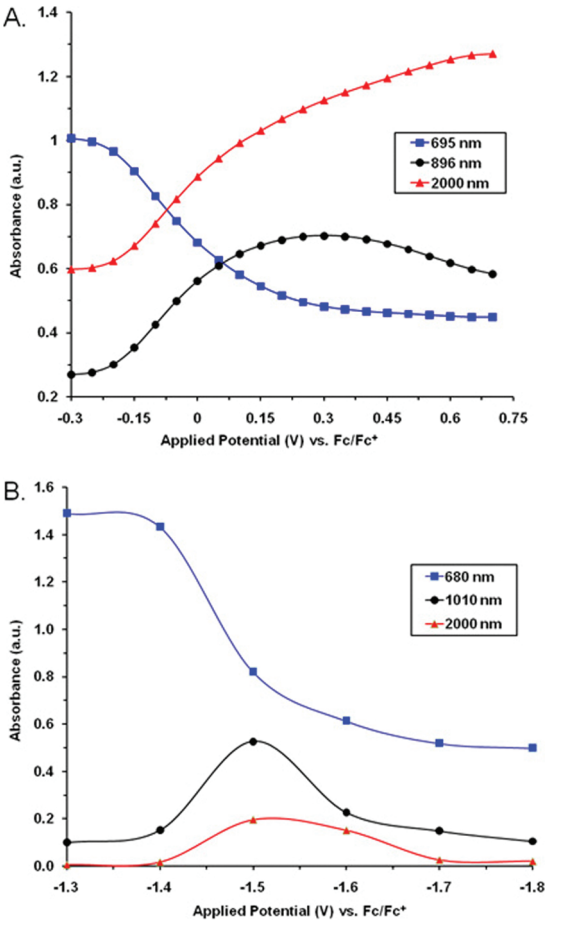

Figure 6. Absorbances in the visible and near-infrared (wavelengths indicated) as a function of applied potential on (A) oxidation and (B) reduction for electropolymerized films of poly(bisEDOT-PyrPyr-Hx$_2$) on SWNT/glass electrodes.

and NIR (896 and 2000 nm) are monitored as a function of potential. The spectra looks near-identical to that performed on ITO with electronic transitions occurring at the same wavlengths, as is expected.

On *n*-doping (Figure 5B), the neutral polymer absorptions decrease with a large contrast in the visible region, while there is a low contrast in the NIR. This small NIR absorbance change occurs with a slight increase in absorbance between the applied potentials of −1.3 to −1.5 V. As further negative potentials are applied to the film, the NIR absorbances begin to decrease. To further clarify, absorbances at the NIR wavelengths of 1010 and 2000 nm and the visible (680 nm) are plotted versus applied reduction potential in Figure 6B. As can be seen in this plot, there is a large drop for the 680 nm wavelength absorbance when the potential is stepped from −1.4 to −1.5 V. In that same potential step, the largest increases for the 1010 and 2000 nm absorbances occur. As the applied potential is made further negative, the visible region absorbance continues to decrease, as do the longer wavelength absorbances. This low NIR contrast is not unexpected as reduction of the polymer creates a radical anion with the negative charge highly localized on the acceptor, resulting in a decreased contrast at lower energies, indicative of limited polymer conductivity as has been noted previously in similar systems.[8] As the second reduction process is not stable, applied potentials were maintained within the first reduction potential window of −1.3 to −1.8 V vs Fc/Fc$^+$.

An important characteristic we have first observed for this polymer is the presence of a lower energy absorption state of the neutral polymer film. Observation of this state occurred upon electrochemically cycling the polymer film in electrolyte solution followed by holding the film at a neutralizing potential of −0.3 V vs Fc/Fc$^+$ for several minutes. Upon measuring the UV/vis-NIR absorbance of the polymer film while this potential is applied, we observed the absorption peak shifted to lower energies from that observed when −1.1 V was applied. This can clearly be seen in Figure 7 where the onset for absorption for a film on SWNT/glass, held at −0.3 V, occurs at 1130 nm, with a λ_{max} at 810 nm. Importantly, this lower energy electronic transition occurs without the longer wavelength carrier induced absorbances in the 1200 to 2000 nm range characteristic of partially doped films that are attributed to polarons. Returning the potential to −1.1 V causes the spectrum to revert to its original form, indicating that the phenomenon observed is fully reversible. Given that all measurements are performed in an inert

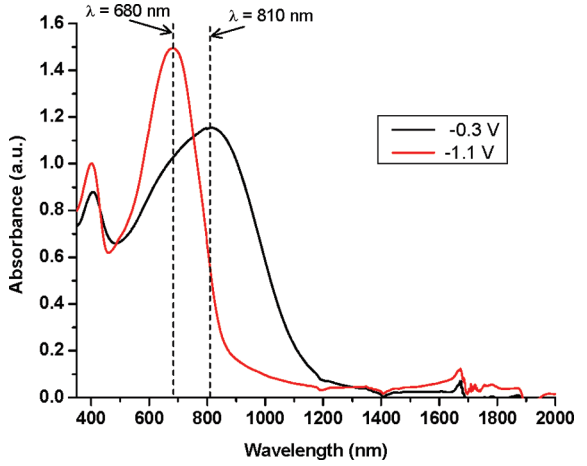

Figure 7. Comparison between a film of poly(bisEDOT-PyrPyr-Hx_2) on a SWNT/glass electrode held at −0.3 V vs Fc/Fc^+ and −1.1 V vs Fc/Fc^+ in 0.2 M TBAP/PC. Both measurements were taken after repeated cycling (between the voltages of −0.6 and 0.6 V vs Fc/Fc^+) of the film and holding at the potential indicated during measurement.

atmosphere glovebox, that the −0.3 V applied to the film is outside the occurrence of a faradaic redox process (as can be seen in Figure 2), and that there is no presence of absorption features indicative of a doped film, we conclude that this lower energy absorption is not due to a partially oxidized polaron state but rather a second neutral state of the polymer film.

We speculate that this spectral shift on application of the voltages from −1.1 to −0.3 V is due to electric field induced solvent and ion reorganization within the polymer film. While it is beyond the scope of this paper to evaluate this process in detail, it is possible that the polymer chain relaxes to a more planarized conformation at the less negative potential yielding a longer average conjugation length and a lower energy absorbance. We have found that inducing this higher energy absorption requires the potential of at least −1.1 V to be held for a sufficient length of time (~20 min) to ensure that the polymer film is fully intercalated with charge-balancing cations as the ions and solvent diffuse into the film quite slowly. Independent of the mechanism of this spectral shift, we are able to capitalize on this lower energy neutral state in creating low bandgap dual- and single-window electrochromic devices utilizing SWNT films as transparent electrodes.

Single-Window Electrochromic Devices. ECDs that operate in a complementary transmissive/absorptive mode consist of two electrochromic material films deposited on transparent electrodes. Devices containing conjugated polymers as both electrochromic materials are typically called "dual polymer ECDs" as both films contribute to the optical properties of the device. To obtain a device that switches between a transparent (bleached) and absorptive state, it is necessary to have an anodically coloring polymer at one electrode and a cathodically coloring polymer at the other with each material complementing the absorption profile of its partner. However, it would be advantageous if the *same* electrochromic polymer could be utilized at both electrodes in a window device, with one side being oxidized (*p*-doped) and the other reduced (*n*-doped). This approach allows for the possibility of a single-spectrum, color pure device in the neutral state, rather than the typically less than perfect overlapping spectra of two different electrochromic materials that together yield a reduced color purity. For a preliminary look at whether the same material can be used as both the anode and the cathode, a modified dual-electrode, although single-window, device was constructed as is described below.

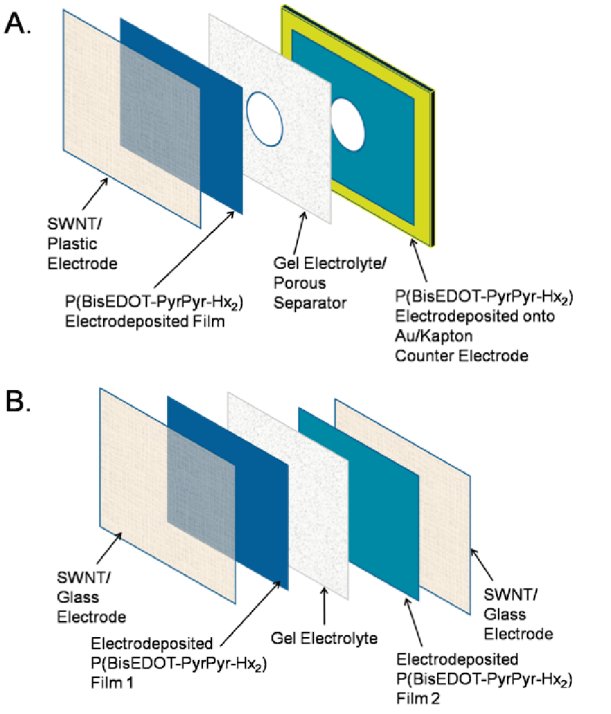

Figure 8. Device schematics for (A) the single-window ECD and (B) the dual-window ECD devices used in this study.

The device schematic for the single-window ECD is shown in Figure 8A. This device contained a SWNT film on PET as the working electrode. Poly(bisEDOT-PyrPyr-Hx_2) was electrochemically deposited, as described previously, to a thickness of 150−200 nm. As the goal of this device was to take advantage of the red-shifted absorbance of the polymer in the lower energy neutral state, the film was held at −0.3 V vs Fc/Fc^+ before device assembly. The counter electrode in this device was a gold-coated Kapton film onto which the same polymer (poly(bisEDOT-PyrPyr-Hx_2)) was deposited. Because the Au/Kapton electrode is not transmissive, a hole—approximately 4 mm in diameter—was cut into the middle of the electrode to allow for transmission measurements to be performed. To prevent electrical shorts from occurring between the working and the counter electrode, a porous filter paper was placed between the two electrodes. A hole was also cut into this separator to prevent it from blocking the light. A layer of gel electrolyte was applied between the two electrodes. To encapsulate the device, a transparent window comprised of PET was applied over the cut hole, and all edges were sealed with epoxy before the device was removed from the glovebox.

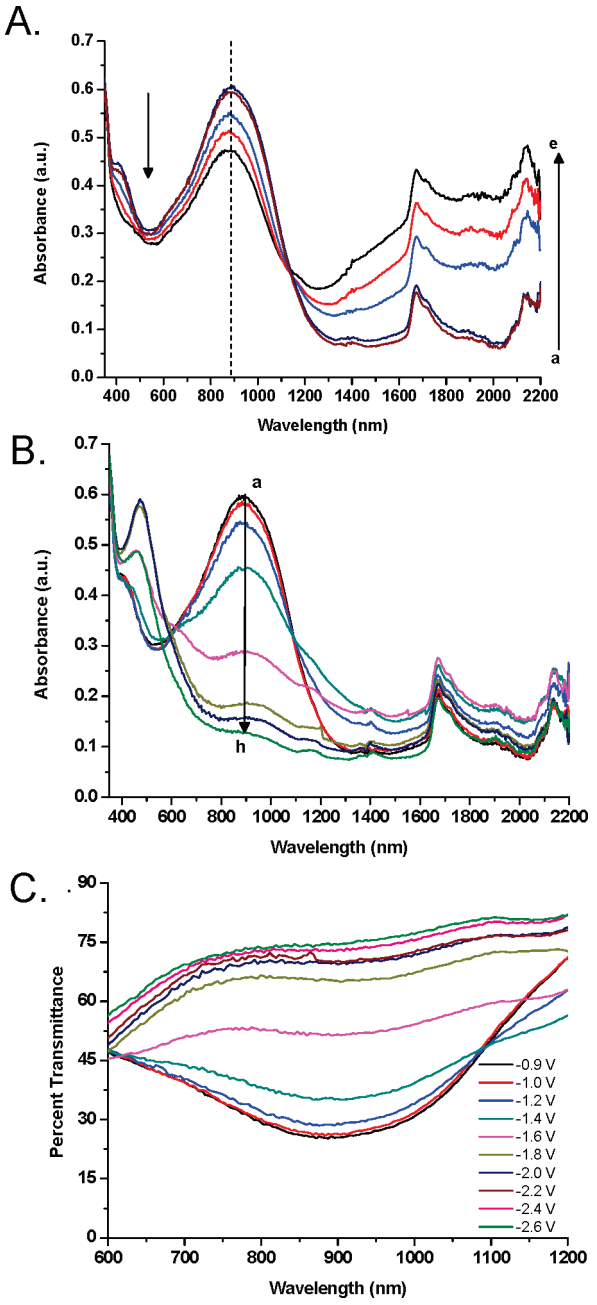

Figure 9. Spectra of a single-window ECD with poly(bisEDOT-PyrPyr-Hx_2) on SWNT/PET as (A) the *p*-doping material and poly(bisEDOT-PyrPyr-Hx_2) on Au/Kapton as the *n*-doping material between the applied cell voltages of (a) −0.5 V; (b) −0.3 V; (c) +0.7 V; (d) +0.8 V; and (e) +0.9 V and (B) the *n*-doping material and poly(bisEDOT-PyrPyr-Hx_2) on Au/Kapton as the *p*-doping material between the applied cell voltages of (a) −0.9 V and (b−h) −1.0 V to −2.6 V at 0.2 V steps. (C) The *n*-doping spectra plotted to highlight the large %T contrast between the wavelengths of 600 to 1200 nm.

The absorbance spectra of the single-window device are shown in Figure 9. As can be seen in Figure 9A, upon application of cell voltages between −0.5 and 0.9 V, the poly(bisEDOT-PyrPyr-Hx_2) film at the SWNT electrode is switched from its neutral state to an oxidized state. It can be seen that the neutral state spectrum corresponds to the peak observed for the more delocalized neutral state observed in Figure 7 and discussed previously. During this oxidation, the electrochromic contrast ($\Delta\%T$) at λ_{max} in the visible region is rather small, with a value of 9%,

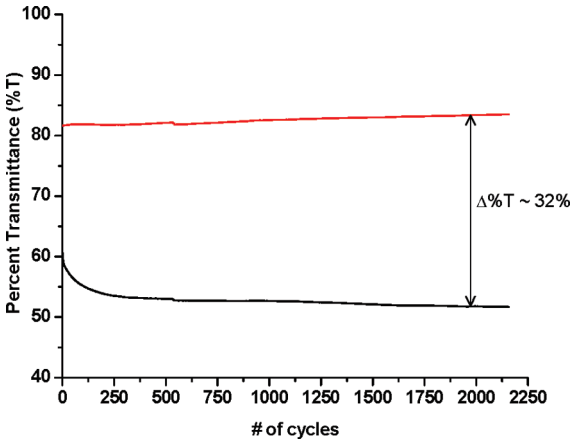

Figure 10. Light transmittance at 2000 nm of a single-window ECD containing poly(bisEDOT-PyrPyr-Hx_2) on SWNT/PET as the oxidizing material and poly(bisEDOT-PyrPyr-Hx_2) on Au/Kapton as the reducing material for applied cell voltages of −0.3 and 0.9 V during continuous cycling for over 2000 switches. The red line traces the maximum in transmittance measured at −0.3 V and the black line traces the minimum in transmittance measured at 0.9 V.

while in the NIR, the contrast is encouragingly higher with a value of 43% at 2000 nm. It can be seen that the neutral polymer transition is not fully depleted, as expected for this experiment where we focused on NIR contrast. This depletion is only expected to occur if the cell voltage is pushed to higher values (> 0.9 V).

The bias across the device was then switched such that the film being measured optically, the poly(bisEDOT-PyrPyr-Hx_2) on the SWNT/PET electrode, was being reduced while the film at the counter electrode (with the hole in it) was oxidizing, providing charge balance. As can be seen in Figure 9B, there is near complete bleaching of the neutral polymer absorption with an electrochromic contrast at 890 nm of 48% when cell voltages of −0.9 V to −2.6 V are applied. This behavior is clearly seen in Figure 9C, where the transmittance is plotted between wavelengths of 600 to 1200 nm. However, the electrochromic contrast in the NIR is minimal (3%) when the device is switched between the two extreme voltages where the film is either neutral or reduced. As with the polymer film during the reduction process, shown in Figures 5B and 6B, the absorbance in the NIR is initially low and increases at intermediate voltages and then returns to a minimal value when the film is fully reduced.

Long-term switching stability measurements were performed on the single-window device when switched between −0.3 and 0.9 V with the contrast at 2000 nm monitored. As shown in Figure 10, the initial contrast at that wavelength was 21%. After 2100 cycles, the contrast has actually increased to 32%. This type of "break-in" is typical of electrochromic devices and, as such, is not surprising. These results demonstrate that the device has a high lifetime stability when the working electrode (poly(bisEDOT-PyrPyr-Hx_2) on SWNT) is switched between a neutral state and fully oxidized state while the counter electrode (poly(bisEDOT-PyrPyr-Hx_2) on Au/Kapton) is switched from a neutral state to the first reductive state.

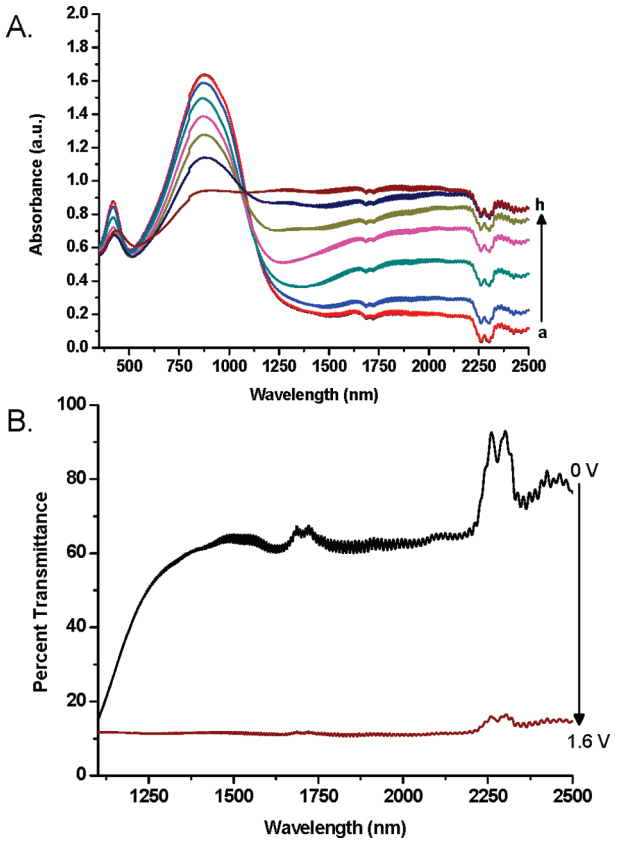

Figure 11. Spectra of a dual-window SWNT ECD with poly(bisEDOT-PyrPyr-Hx$_2$) as both the *n*-doping and *p*-doping electrochromic materials at applied cell voltages of (a) 0 V and (b−h) +0.4 V to +1.6 V at 0.2 V steps and (B) the same device showing the transmittance contrast between 1100 and 2500 nm at 0 V and 1.6 V.

Dual-Window Electrochromic Devices. The ultimate goal of this study was construction of dual-window EC devices utilizing poly(bisEDOT-PyrPyr-Hx$_2$) as the electrochromic polymer on both working and counter electrodes. The structure of this device is as shown in Figure 8B and consists of two poly(bisEDOT-PyrPyr-Hx$_2$)-coated SWNT/PET electrodes facing each other. The SWNT/PET electrodes are transparent from the visible to mid-infrared region. The polymer films are separated by a thin layer of gel electrolyte. The two polymer films in the device were in the same neutral state when the device was assembled. When a zero bias is applied across the device, both polymers are in the neutral state with the absorbance onset at ~1200 nm and peak ~800 nm. As an increasing bias is applied across the device, one polymer becomes oxidized while the other is reduced.

The absorbance of the dual window poly(bisEDOT-PyrPyr-Hx$_2$) ECD was measured from the visible to near-infrared region for applied voltages of 0.0 to 2.6 V. These results are shown in Figure 11A, as the absorbance of the dual window ECD, at voltages from 0.0 to 1.6 V. When both films are in the same, neutral state, the overall absorbance is additive. When the cell voltage is 0 V, the absorbance onset and λ_{max} is in the same region as with the single window device, although the absorbance value is increased to ~1.7 absorbance units from ~0.6 units. As the cell voltage is increased to 1.6 V, the absorbance in the visible region decreases, while those in the NIR increase. The optical contrast over this voltage range is 9% at 875 nm (λ_{max}) and 52% at 2000 nm. Figure 11B shows this clearly as the transmittance contrast of the device between the wavelengths of 1100 and 2500 nm. As was seen in the individual films, when the voltage across the device is increased from 1.6 to 2.6 V, the NIR absorbances begin to decrease (not shown). As the SWNT films are highly transparent—and the polymer is expected to have electrochromic contrasts at wavelengths longer than what was accessed here—it is expected that the devices can be utilized into the mid- and far-IR regions of the spectrum.

Conclusions

The redox electrochemistry and electrochromism of a donor−acceptor−donor linked conjugated polymer, poly(bisEDOT-PyrPyr-Hx$_2$), is reported. In addition to stable oxidation and reduction (*p*- and *n*-type doping) processes, this polymer exhibits a neutral state with a lower-energy absorption onset at 1200 nm and a second neutral state with a higher energy absorption onset due to a shorter conjugation length (presumably due to cation intercalation inducing a torque within the polymer chain). Single-window and dual-window SWNT electrochromic devices were constructed in which the same polymer acts as anode and cathode, similar to Type III supercapacitor devices, simplifying device construction and resulting in a clean optical spectrum in the neutral state, something not achievable with devices containing two different polymer films. The single-window devices exhibited large contrasts in the NIR (~40%) and visible (~50%) and long-term switching stability of over 2100 cycles. The dual-window electrochromic device exhibited large NIR contrasts (> 50%) out to 2500 nm. To our knowledge, this is the first report of a SWNT dual-window electrochromic device containing the same polymer at both electrodes where one layer is oxidized while the other is subjected to reductive redox processes. Further work in this area is directed toward new device designs that would allow for even higher optical contrasts in the visible and NIR while utilizing SWNT electrodes for modulation of even longer wavelengths of light.

Acknowledgment. We gratefully acknowledge funding from the Office of Naval Research (N00014-08-1-0928) and Nanoholdings, LLC.